Investigation of the Flow in the Vicinity of an Isolated 3D Surface Roughness

Anke Wörner, Ulrich Rist, and Siegfried Wagner

Universität Stuttgart, Institut für Aerodynamik und Gasdynamik
Pfaffenwaldring 21, D-70550 Stuttgart, Germany

Summary

In the present paper, a detailed numerical investigation of the flow field in the vicinity of an isolated 3D surface roughness is presented. The Direct Numerical Simulations (DNS) shown are based on the velocity-vorticity formulation of the complete Navier–Stokes equations for incompressible fluids. The small surface roughness is modeled within the cartesian grid using an immersed boundary technique.

In the wake of the surface irregularity, a pair of counter-rotating streamwise vortices is visible at each side of the roughness. The pair of vortices results in a high-speed streak downstream of the spanwise edge of the roughness, which is flanked by two low-speed streaks. The whole vortex system looks very similar to horseshoe vortex systems that were observed in experiments around surface mounted cylinders or cubes.

1 Introduction

The specific fuel consumption of any aircraft is directly related to its drag. A major portion of aircraft drag is due to friction which is confined to the wall boundary layer of the flow. Since a turbulent boundary layer produces higher skin friction than a laminar one, the overall skin friction is highly influenced by the location of laminar-turbulent transition. By means of control (i.e. delay) of laminar-turbulent transition a reduction of the wall friction is possible. A better understanding of the mechanisms of laminar-turbulent transition is the key for being able to actively or passively delay transition on an airfoil.

The process of laminar-turbulent transition can be subdivided into four main stages. The first stage, the so called receptivity, is the penetration of external perturbations into the boundary layer where they are tuned to boundary layer disturbances. The second stage is the linear amplification of these initially created disturbances, the third one is the nonlinear development and the last one the breakdown to turbulence. This process of transition from the laminar to the turbulent state may be influenced by external perturbations in the freestream such as vortices, sound, entropy or particles as well as by internal perturbations in the boundary layer itself such as vibrations or surface non-uniformities.

In the manufacturing process of an airfoil, surface discontinuities such as steps at junctions or small humps are unavoidable. Additionally, surface roughness may be caused by contamination of the airfoil surface by insects, ice or mud. All these surface discontinuities can influence the location of transition on the airfoil via two dominating mechanisms. First, they are possible sources of receptivity, which means that they provide the small length scale which is necessary for the conversion process of large scale external perturbations into small scale boundary layer disturbances (see [1], [2] or [4]). A second aspect is however, that they are also able to either locally stabilize or destabilize the boundary layer.

The study presented here shall provide a first insight into the influence of an isolated 3D surface non-uniformity on the transition process. As a first step, the perturbations that are created by the presence of the surface non-uniformity itself are studied in detail using direct numerical simulations.

2 Numerical Method

The DNS code used for the present investigation is based on a code first developed by Fasel and further improved by Rist, Kloker et al., which is used for the investigation of transition phenomena on a flat plate.

The code is based on the velocity-vorticity formulation of the complete Navier–Stokes equations for incompressible fluids. The flow field is discretised using sixth order accurate compact finite differences in streamwise (x-) and wall-normal (y-) direction. An equidistant grid is used in x-direction, whereas grid stretching is applied in y-direction, leading to a very fine grid in the near wall region. In spanwise (z-) direction a spectral representation of the flow field is used. The time integration is done using a fourth order, four step Runge–Kutta scheme. A sketch of the integration domain including a buffer domain at the outflow boundary to avoid reflections at this boundary is shown in figure 1.

The localised surface irregularity within the cartesian grid is modeled using a technique which is related to Peskin's immersed boundary approach [8], and which has already successfully been applied for example by Goldstein et al. [3], Linnick [7] or von Terzi et al. [10]. In this approach, the effect of the surface irregularity on the surrounding flow field is modeled with an external force field which enforces no-slip and no-through-flow at selected grid points or at selected points between the grid points at every time step.

The vorticity transport equations with an external force field $\boldsymbol{F} = (F_x, F_y, F_z)$ can be written as

$$\begin{aligned}
\frac{\partial \omega_x}{\partial t} + \frac{\partial}{\partial y}(v\omega_x - u\omega_y) - \frac{\partial}{\partial z}(u\omega_z - w\omega_x) &= \frac{1}{Re}\Delta\omega_x + \frac{\partial F_y}{\partial_z} - \frac{\partial F_z}{\partial y} \\
\frac{\partial \omega_y}{\partial t} - \frac{\partial}{\partial x}(v\omega_x - u\omega_y) + \frac{\partial}{\partial z}(w\omega_y - v\omega_z) &= \frac{1}{Re}\Delta\omega_y + \frac{\partial F_z}{\partial_x} - \frac{\partial F_x}{\partial_z} \\
\frac{\partial \omega_z}{\partial t} + \frac{\partial}{\partial x}(u\omega_z - w\omega_x) - \frac{\partial}{\partial y}(w\omega_y - v\omega_z) &= \frac{1}{Re}\Delta\omega_z + \frac{\partial F_x}{\partial y} - \frac{\partial F_y}{\partial x}
\end{aligned} \tag{1}$$

Here u,v and w denote the streamwise, wall-normal and spanwise velocity components and ω_x, ω_y and ω_z the streamwise, wall-normal and spanwise components of vorticity. t denotes the time and Re is a Reynolds number which is determined by the choice of the reference length and velocity used for non-dimensionalisation.

The force term on the right hand side is the force exerted by the surface irregularity on the fluid and can be written as

$$\boldsymbol{F} = \oint \boldsymbol{f}(\boldsymbol{x}_S, t) \cdot \delta(\boldsymbol{x} - \boldsymbol{x_S})\, dS. \tag{2}$$

For numerical reasons, the delta function is approximated by a Gaussian function as follows:

$$\delta \approx e^{-\left(\frac{x-x_S}{\sigma_x}\right)^2 - \left(\frac{y-y_s}{\sigma_y}\right)^2 - \left(\frac{z-z_s}{\sigma_z}\right)^2} \tag{3}$$

The surface body force $\boldsymbol{f}$ is determined from the relation

$$\boldsymbol{f}(\boldsymbol{x_S}, t) = \alpha_S \cdot \int_0^t \boldsymbol{v}(\boldsymbol{x}_S, t')\, dt' + \beta_S \cdot \boldsymbol{v}(\boldsymbol{x}_S, t) \tag{4}$$

for surface points $\boldsymbol{x}_S$, velocity $\boldsymbol{v}$, time t and negative constants α_S and β_S which represents a feedback scheme in which the velocity is used to iteratively approach the desired value.

If the surface of the irregularity is located between the grid points, the velocity at this location is interpolated from the values at the neighbouring grid points using a 4th order Lagrangian interpolation procedure.

Considering the fact that a spectral representation of the flow field in spanwise direction is used for the present investigation, it is clear, that, introducing point forces into such a scheme will cause some numerical problems. These result from the fact that singularities tend to produce significant spatial oscillations even in a temporally steady flow and have already been encountered by Goldstein et al. [3]. To eliminate these oscillations, a mild spectral smoothing in spanwise direction is applied. The spectral coefficients of the vorticity components are multiplied by

$$e^{-(k/K)^{20}}, \tag{5}$$

where k is the grid point index in spanwise direction and K the number of Fourier modes used in this direction. This is a low-pass filter. The decay constant of 20 is chosen so that there will be a sharp cut-off of the highest modes and so that the highest wavenumber will be reduced by $1/e$. Of course, with higher resolution this smoothing will have less influence on the flow and will probably no longer be necessary if a really huge resolution could be used. The maximum resolution used in the present investigation was restricted by the available amount of memory and computation time. The resolution used can be described as follows: The height of the integration domain is about 4 times the boundary layer thickness at the inflow boundary, its length about 45 times and its width about 8 times the radius of the roughness element. The number of grid points is 1802 in streamwise and 193 in wall-normal direction. In spanwise direction 80 Fourier modes are used.

3 DNS Results

As a first step towards receptivity calculations, the flow field in the vicinity of a localised, three-dimensional roughness element on a flat plate was calculated and investigated in detail. The surface irregularity is located at $x = 2.471$, which corresponds to $Re_{\delta_1} = 855$ for the undisturbed flow (Blasius: $Re_{\delta_1} = \sqrt{Re \cdot x}$). It's height, non-dimensionalised with the local displacement thickness of the undisturbed boundary layer at the location of the irregularity, is $h/\delta_1 = 0.5$. The surface roughness is rotationally symmetric with a radius of $b/\delta_1 = 8.42$ and the following shape:

$$h(x,z) = h_0 \cdot cos^3 \left(\frac{\pi r}{2b} \right) \tag{6}$$

with

$$r = \sqrt{(x - x_1)^2 + z^2}. \tag{7}$$

Here x denotes the streamwise and z the spanwise coordinate, h_0 is the maximum height in the center of the roughness, b the radius of the roughness and x_1 denotes the distance of the center of the roughness from the leading edge of the flat plate. In spanwise direction, the roughness is located at $z_1 = 0$. The shape of the surface irregularity under investigation is illustrated in figure 2. First calculations showed that a very fine spatial resolution, especially in the vicinity of the surface non-uniformity was absolutely necessary to gain reasonable results. This led to the use of grid stretching in wall-normal direction to keep the computational effort within a reasonable range.

What we observe in our DNS up to now is that the flow field in the vicinity of the surface irregularity is governed by the following features: In the wake of the surface irregularity a pair of counter-rotating vortices is visible on each side of the roughness. The outer vortex seems to originate directly upstream of the roughness and seems to be wrapped around in a similar way as a horseshoe vortex. The inner vortex seems to originate downstream of the outer one at the spanwise edge of the roughness element. The whole flow pattern looks very similar to horseshoe vortex systems that were observed in experiments around surface mounted cylinders or cubes (see [9]). A visualisation of the vortical structures in the flow field using the λ_2-method [5] is shown in figure 3. To provide a better insight into the details of the flow field in the near wall region, the wall-normal direction is stretched by a factor of 5. Figure 4 shows selected streamlines together with contours of the streamwise velocity component u in zy-planes. The y-direction is again stretched, in contrast to the previous plot, this time by a factor of 10. The illustration shows, that the pair of vortices results in a high-speed streak downstream of the spanwise edge of the roughness, which is flanked by two low-speed streaks. In the middle of the two counter-rotating vortices, high speed fluid from the outer region of the boundary layer is transported towards the wall, whereas on the outer edge of the two vortices, low speed fluid from the near wall region is transported away from the wall. This can be seen more clearly in a cutting plane shown in figure 5 located at $x = 2.57$, downstream of the roughness, where the location of the vortices (visualised by contours of the streamwise vorticity ω_x) is compared to the location of the streaks (visualised by contours of u', i.e. the deviation of u from the value for a flat plate without roughness). Here, solid lines denote positive values of u' (acceleration) and dashed lines negative values (deceleration). One can clearly see, that the high-speed streak is located in the middle of the vortices, whereas the low-speed streaks are located on the outer edges. An additional observation is, that all disturbances created by the presence of the surface irregularity are limited to the region downstream of the roughness, which means that they do not spread in spanwise direction. This observation is illustrated in figure 6, where ω_z at the wall is plotted versus x and z. It is in agreement to experimental findings reported by Kendall in [6].

4 Conclusion

As a first step towards calculations on non-linear 3D roughness receptivity, the flow field in the vicinity of a localised 3D surface non-uniformity was studied in detail using direct numerical simulations. For the modeling of the surface non-uniformity, an immersed boundary technique was applied.

By the presence of the surface non-uniformity, a pair of counter-rotating streamwise vortices was formed on each spanwise edge of the roughness element. Each pair of vortices resulted in a high-speed streak in the middle of the two vortices flanked by two low-speed streaks on the outer edges. The vortex system, that was generated by the presence of the localised surface non-uniformity, looked very similar to horseshoe vortex systems observed in experiments in the vicinity of surface mounted cylinders or cubes.

Acknowledgements

The financial support by the German Research Council (DFG) under contract number Ri 680/7-2 is gratefully acknowledged. The computations were carried out at the HLRS Stuttgart on a NEC SX-5.

References

[1] M. Choudhari and C.L. Streett: "A finite Reynolds-number approach for the prediction of boundary-layer receptivity in localized regions". Phys. Fluids, A **4**, 1992, pp. 2495-2514.

[2] J.D. Crouch: "Localized receptivity of boundary layers". Phys. Fluids, A **4**, 1992, pp. 1408-1414.

[3] D. Goldstein, R. Handler and L. Sirovich: "Modeling a no-slip flow boundary with an external force field". J. Comp. Phys., **105**, 1993, pp. 354-366.

[4] M.E. Goldstein: "Scattering of acoustic waves into Tollmien-Schlichting waves by small streamwise variations in surface geometry". J. Fluid Mech., **154**, 1985, pp. 509-529.

[5] J. Jeong and F. Hussain: “On the identification of a vortex”. J. Fluid Mech., **285**, 1995, pp. 69-94.
[6] J.M. Kendall: “Laminar boundary layer velocity distortion by surface roughness: effect upon stability”. AIAA-Paper 81-0195.
[7] M.N. Linnick: “Investigation of actuators for use in active flow control”. M. Sc. Report, University of Arizona, 1999.
[8] C.S. Peskin: “Numerical analysis of blood flow in the heart”. J. Comp. Phys., **25**, 1977, pp. 220-252.
[9] R. Sedney: “A survey of the effects of small protuberances on boundary-layer flows”. AIAA Journal, vol. **11**, no. 6, 1973, pp. 782-792.
[10] D.A. von Terzi, M.N. Linnick, J. Seidel and H. Fasel: “Immersed Boundary Techniques for High-Order Finite-Difference Methods”. AIAA-Paper 2001-2918.

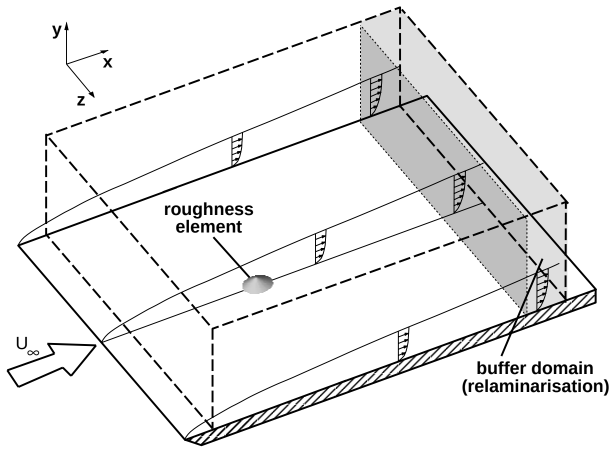

Figure 1 Sketch of the integration domain

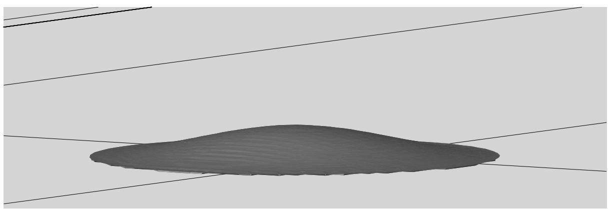

Figure 2 Shape of the localised roughness element; wall-normal direction stretched by a factor of 2 in relation to streamwise and spanwise direction

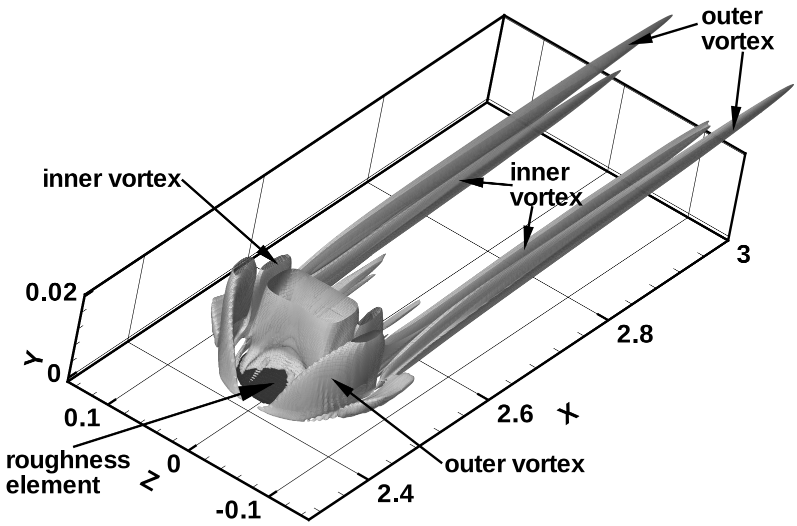

Figure 3 Flow field in the vicinity of a localised hump, located at $x = 2.471$, with $h = 0.004275$, $b = 0.072$; visualisation of the vortex system generated by the localised hump by a λ_2-Isosurface ($\lambda_2 = -1$); y-direction stretched by a factor of 5 in relation to x- and z-direction

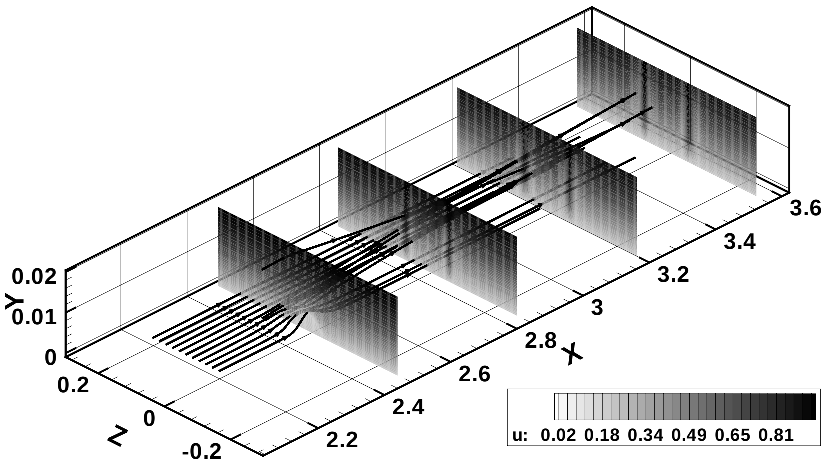

Figure 4 Flow field in the vicinity of a localised hump, located at $x = 2.471$, with $h = 0.004275$, $b = 0.072$; selected streamlines and contours of the streamwise velocity u in zy-planes; y-direction stretched by a factor of 10 in relation to x- and z-direction

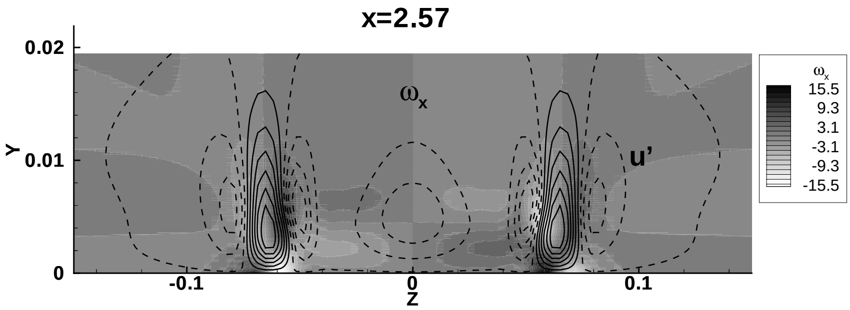

Figure 5 Comparison of ω_x-contours with u'-contours downstream of the surface non-uniformity at $x = 2.57$; solid lines: positive values of u', dashed lines: negative values of u'

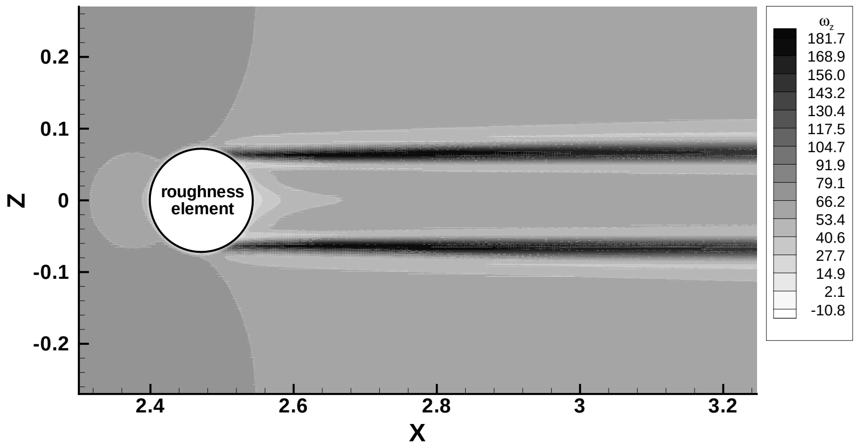

Figure 6 Contours of ω_z at the wall ($y = 0$); surface non-uniformity located at $x = 2.471$, $z = 0$